Origin of dielectric relaxations in polycrystalline $RbHSeO_4$ above room temperature

O. Checa[a], R. A. Vargas[b] and J. E. Diosa[b]
[a]*Departamento de Ciencias Básicas, Universidad Nacional de Colombia, Palmira, Colombia.*
e-mail: oychecac@unal.edu.co
[b]*Departamento de Física, Universidad del Valle, A.A. 25360, Cali, Colombia.*

Received 6 May 2013; accepted 24 July 2013

In the present paper, the dielectric relaxation properties of $RbHSeO_4$ have been studied by means of impedance spectroscopy measurements over wide ranges of frequencies at several isotherms (T<415 K). The frequency dependence of the permittivity data reveal a distinct dielectric relaxation at low frequency, which is about 385 Hz at 310 K, then it shifts to higher frequencies (∼40 kHz) as the temperature increases. The $f_{\max}$ vs. reciprocal T shows an activated relaxation process with an activation energy of 0.9 eV, which is in close agreement with that associated with transport of charge carriers. We suggest that the observed dielectric relaxation could be attributed to polarization induced by the proton jump and selenate tetrahedral reorientations. The displacement of mobile H^+ proton accompanied by SeO_4^{-2} tetrahedra reorientations create structural distortion in both sublattices which induce localized dipoles like $HSeO_4^-$.

Keywords: Ionic conductivity; dielectric relaxations.

PACS: 67.25.du; 77.22.Gm; 72.50.b; 73.61.Jc

1. Introduction

Rubidium hydrogen selenate ($RbHSeO_4$) belongs to the $MHXO_4$ family compounds (M = Rb, Cs, K, NH_4 and X = S, Se), that has been widely studied because of its high proton conductivity and its phase transition phenomena [1-4]. This family forms an interesting group of materials characterized by the presence pattern of hydrogen bonding between the HXO_4^- tetrahedral ions [1-4]. The structures of $RbHSeO_4$ and NH_4HSeO_4 are found to be very similar in corresponding phases [5-8]. However, NH_4HSeO_4 exhibits an incommensurate phase over ten degrees between the ferroelectric and the paraelectric phases [9,10]. Such incommensurate phase has not been found in $RbHSeO_4$, which at 371 K [11] jumps directly from the ferroelectric triclinic phase [5,8] to the paraelectric monoclinic phase [6,8]. In the triclinic phase, near the phase transition, dielectric properties and Brillouin scattering results have revealed an anomaly at the dielectric and elastic constants [12-14].

Research has been devoted to understand the dynamics of ionic transport in solid ionic conductors. Most research activity in this field has focused on the origin and properties of the ion motions, and electrical relaxation is the most commonly used experimental tool to access the ion dynamics.

Complex impedance methods have successfully been used to measure the conductivity of liquid and solid electrolytes in the low frequency range, typically from 0.1 Hz to 1 MHz, which corresponds to "long range" charge motions while measurements of the dielectric properties up to the GHz range [15-18] can reveal dielectric relaxations associated with local motions (reorientations, ion jumps). In previous work by our research team [19-25], it was observed that the dielectric response of MH_2PO_4 (M=K, NH_4), L_2SO_4 (L=K, Li, Cs, Na) and $CsHSeO_4$, reveal a dielectric relaxation at low frequency, for example for $CsHSeO_4$around 4 kHz at 323 K, which shifts to higher frequencies (∼100 kHz) as the temperature increases. We have suggested that this dielectric relaxation could be due to the proton jump and phosphate or sulphate or selenate reorientations that cause distortion and change the local lattice polarizability inducing dipoles like $H_2\ PO_4^-$ in MH_2PO_4 (M=K, NH_4), LSO_4^- in L_2SO_4 (L=K, Li Cs, Na) and $HSeO_4^-$ in $CsHSeO_4$, respectively. Also, we observed that the substitution of NH_4^+ instead of K^+ only shifts the characteristic relaxation frequency, $f_{\max}$, to slightly higher values.

The aim of our work is to obtain more insight into the low frequency dielectric behavior of $RbHSeO_4$, in which the rotation of the $HSeO_4^-$ radicals has been claimed to be important. If the complex permittivity representation of measured dielectric data is used, the real and imaginary parts (ε' and ε") are dependent on each other as inferred from the Kramers-Kronig relations [26]. Such relations evidence the correlations between dispersion (variation of ε' as a function of frequency) and absorption (non-zero value of ε"): any dielectric dispersion is accompanied by an absorption peak. The real and imaginary part of the complex permittivity, ε, can be determined from measured impedance data since

$$\varepsilon' = -\frac{Z''}{\omega C_0 (Z'^2 + Z''^2)} \tag{1}$$

$$\varepsilon'' = \frac{Z'}{\omega C_0 (Z'^2 + Z''^2)} - \frac{\sigma_0}{\omega \varepsilon_0} \tag{2}$$

where $\omega = 2\pi f$ (Hz) is the angular frequency, C_0 is the capacitance of the empty sample cell, σ_0 the dc-conductivity

while Z' and Z'' are the real and imaginary part of the impedance. The last term in Eq. (2) results from the definition of the complex conductivity by the relation $\sigma*(\omega) = \sigma'(\omega) + \sigma_0 + i\sigma''(\omega) = i\omega\varepsilon*(\omega)$, where the real component include the "true dc" conductivity, then, the "dielectric" components are given by $\sigma'(\omega) = \omega\varepsilon''(\omega)$ and $\sigma''(\omega) = \omega\varepsilon'(\omega)$. Since $\varepsilon'(\omega)$is correlated with polarization and $\varepsilon''(\omega)$ with energy losses, then, the dielectric loss contribution due to displacement of charge (last term in Eq. (2)) makes it difficult to detect dielectric relaxations due to dipolar processes in ionic conductors at low frequency. Even if the corrective term in Eq. (2) is properly used, this becomes particularly evident in the present situation in which both terms in Eq. (2) become large at low frequency since $\varepsilon''(\omega)$ is determined by subtracting the two. Due to this, a method based on analyzing the $\varepsilon'(\omega)$ data is also used in this work. We report here results of dielectric relaxation measurements for polycrystalline $RbHSeO_4$ in the 20 Hz to 1 MHz frequency range.

2. Experimental

The polycrystalline $RbHSeO_4$ samples were grown from an aqueous solution of Rb_2CO_3 and $HSeO_4$ by slow evaporation. The electrical measurements were performed using a two-electrode configuration. Cylindrical pellets 0.5 mm thick were prepared for electrical measurements. Platinum electrodes (with diameter 5 mm) were painted at both faces. Impedance spectroscopy measurements were performed by using a LCR meter HP 4284 A, in the frequency range 20 Hz – 1 MHz, and at different temperatures between 31 K and 414 K. The polycrystalline sample were ground mechanical to fine powder for X-ray diffraction identification (XRD). The powder XRD studies were performed using a Philips diffractometer: Panalytical X'Pert PRO MPD, using Cu-K_α radiation (λ = 1.5418 Å, 45 kV and 40 mA).

3. Results and discussion

Figure 1 shows the powder X-ray diffraction patterns for a freshly grown $RbHSeO_4$ sample indicating that it was single phase.

Impedance spectra of the $RbHSeO_4$ samples gave Nyquist plots. Figure 2 shows a typical (ReZ, -ImZ) plot, at some representative temperatures taken between 310 K and 414 K. This spectrum shows two well defined regions: an arc passing through the origin in the high-frequency limit, which is related to the conduction processes in the bulk of the sample, and a monotonically decreasing curve with increasing frequency in the low-frequency limit that is attributed to the charge-transfer processes at the electrodes/sample interface.

Figure 3a) shows the frequency dependence of the real part of the ac conductivity, $\sigma\prime(\omega)$, at several temperatures for the samples under study As expected, we observe an increase of the conductivity as the temperature increases Fig. 3b) shows the amplifications of the isotherms in the temperature

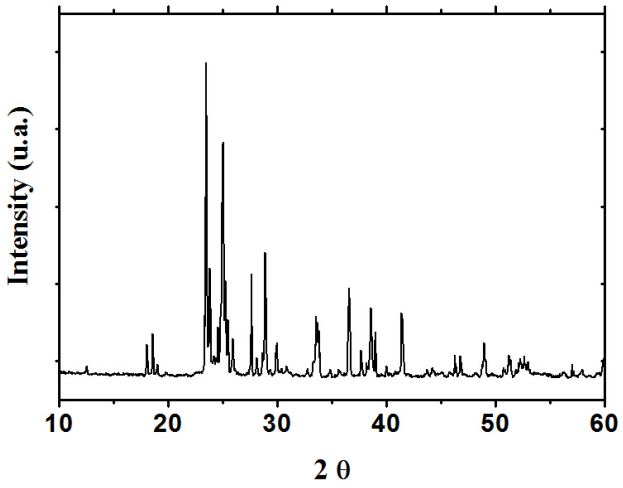

FIGURE 1. Powder X-ray diffraction patterns for a polycrystalline sample of $RbHSeO_4$.

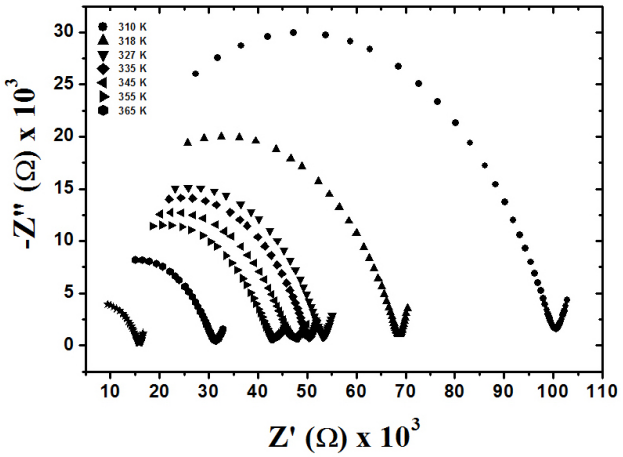

FIGURE 2. Complex impedance (Nyquist) plot for $RbHSeO_4$ between 310 K and 365 K

range from 310 to 365 K in which we can distinguish three dispersive regions with increasing frequency: a low-frequency region I which corresponds to the electrode blocking effects as a consequence of transfer of charge across the electrode/sample interface An intermediate-frequency region II, where the conductivity increases less gradually with increasing frequency, *i.e.* it is not quite direct current (dc) conductivity, as it is frequently seen in other ion-conducting materials [27], that may corresponds to volume low frequency dispersion (LFD) processes [28]. In general, LFD behavior is seen in dielectric systems at low frequencies, in which the ionic carrier responses predominate over the more conventional dipolar effects which ultimately dominate at high frequencies processes. This brings us to the question of the "true dc" component σ_0 to be used in Eq. (2), which, in principle, is dominant at sufficiently low frequencies. The question whether this dc component is experimentally separable from any LFD component is open to debate [28], however, being the "long range" ionic hop the principal transport element in LFD it is expected that the conductivity data in

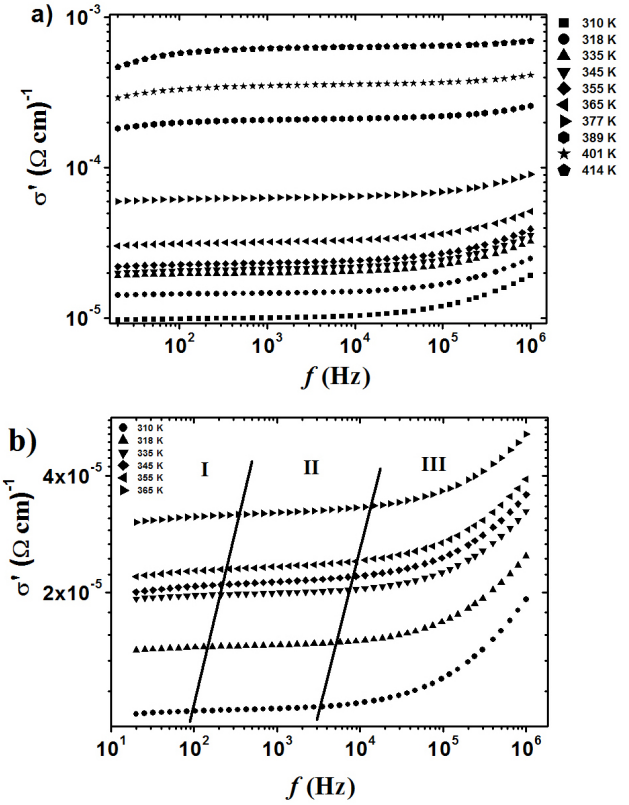

FIGURE 3. Frequency dependence of the real part of the conductivity for $RbHSeO_4$ a) at several temperatures and b) at the temperatures in which three different dispersion regions are identified.

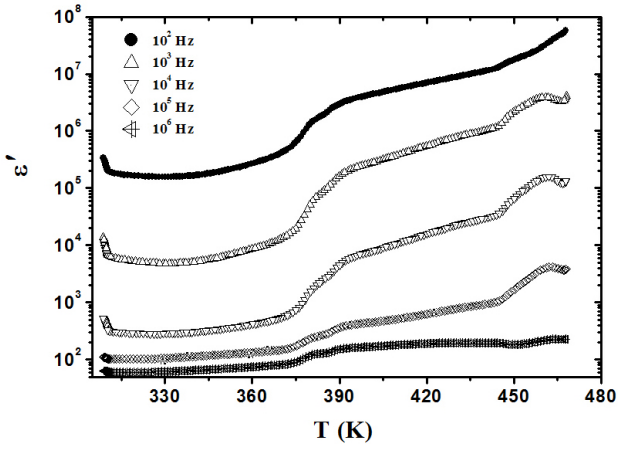

FIGURE 4. Real part of the permittivity $\varepsilon'(T)$ as a function of temperature at several frecuencies for $RbHSeO_4$.

this region is very similar to "true dc" in its activation energy and the magnitude of conductivity associated with it. The high-frequency region III is a more rapidly rising branch which begins at a characteristic frequency f_p that increases with increasing temperature

The temperature dependence of the "near dc" conductivity calculated at the starting point of region II (see Fig. 3b) is plotted in Fig. 5 as a function of reciprocal temperature of

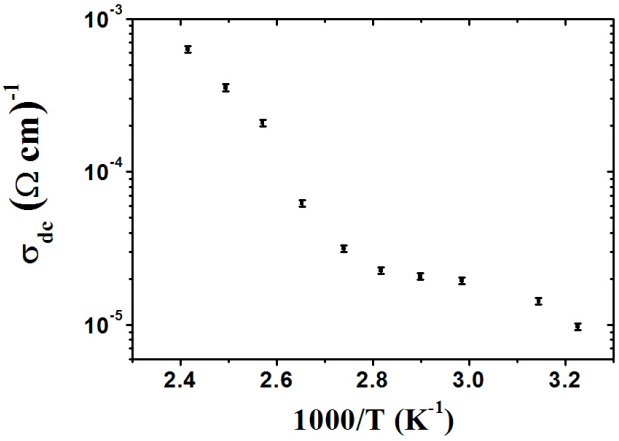

FIGURE 5. Arrhenius Plot of "near dc" conductivity for the sample $RbHSeO_4$, between 310 K and 414 K, during a heating run. σ_{dc} was calculated as discussed in the text.

the sample $RbHSeO_4$. At around 365 K we observed the reported directly jump [11] from the ferroelectric triclinic phase [5,8] to the paraelectric monoclinic phase [6,8] (see Fig. 4). Above 365 K an Arrhenius-type activation process is clearly seen and the activation energy was calculated as 0.8 eV in the temperature range from 365 K to 414 K.

The imaginary part of the relative permittivity after subtracting the "near dc"conductivity contribution, $\varepsilon''(\omega)$, is shown in Fig. 6 as a function of frequency at several isotherms. A broad peak is observed at low frequencies, for example, at 310 K the peak frequency is 385 Hz. The peak shifts to higher frequencies and the peak height decreases as the temperature increases as expected for a dipolar relaxation.

Figure 7 shows the frequency dependence of the real part of the permittivity $\varepsilon'(\omega)$ for various isotherms in log-log plots. Clearly, there is a correlation between the absorption peak observed in the imaginary part of the permittivity data, $\varepsilon''(\omega, T)$ (Fig. 6), and dispersion (step change) in its real part $\varepsilon'(\omega, T)$.

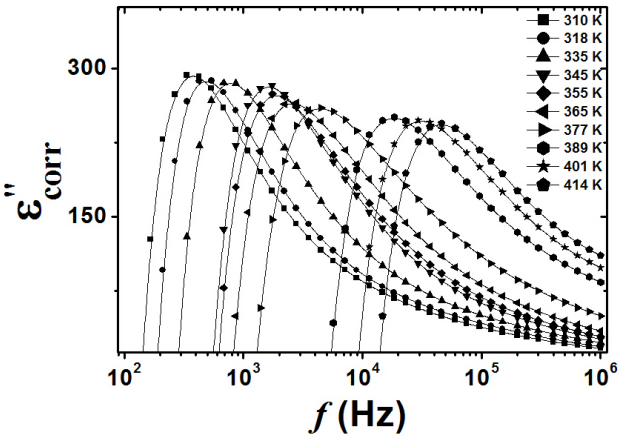

FIGURE 6. Corrected imaginary part of the relative permittivity (after subtracting the "near dc" conductivity contribution), ε"(ω, T), as a function of frequency at several isotherms.

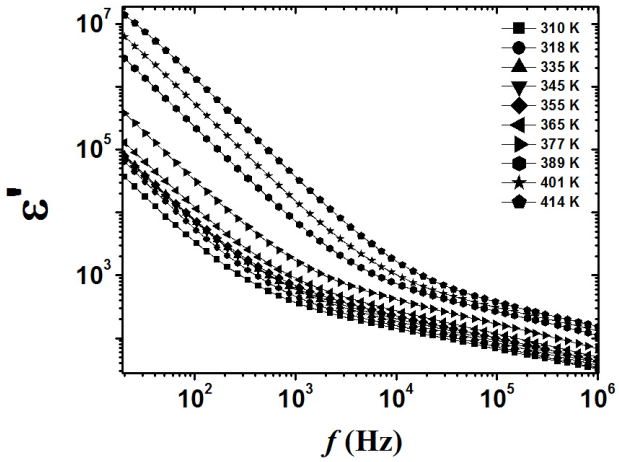

FIGURE 7. Real part of the permittivity $\varepsilon'(\omega, T)$ as a function of frequency at several isotherms (310 K<T<414 K) for $RbHSeO_4$.

The peak frequency, $f_{\max}$, for $RbHSeO_4$ sample (taken from ε" representation) as a function of inverse temperature is shown in Fig. 8. The figure shows that for the sample there is an activated relaxation process (Arrhenius-type) in the temperature range 310 - 414 K with an activation energy, E_a = 0.9 eV, close to the value obtained from the ionic conductivity for the same temperature range (see Fig. 5). This type of low frequency relaxations has to our knowledge not been studied in detail earlier for the $RbHSeO_4$ compound. The relaxation frequencies that we have measured are even lower than that reported for the low frequency relaxation observed by Badot and Colomban [17] in NH_4HSeO_4. In that case the relaxation was assigned to a reorientation of NH_4^+ ions since the ammonium reorientations and the proton displacement may change the local lattice polarizability. According to the Colomban-Novak classification [18], the proton transfer and the HXO_4^- reorientation, take place for frequencies at around 50 MHz and 20 GHz respectively. How

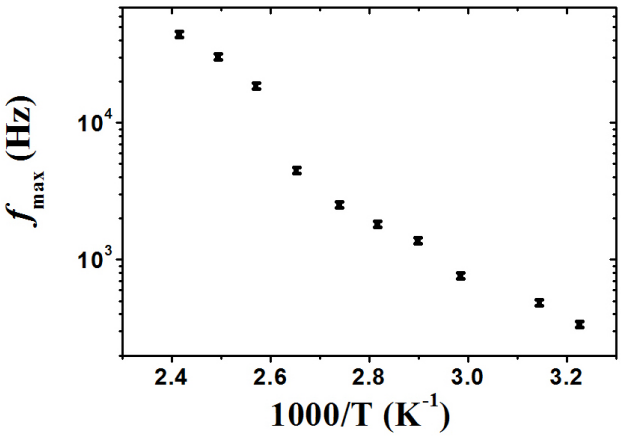

FIGURE 8. Temperature dependence of $f_{\max}$ (taken from ε" representation), plotted as $f_{\max}$vs. 1/T for $RbHSeO_4$.

However, proton dynamics at temperatures below the superprotonic transition (phase II) of $CsHSO_4$ [29,30] studied by proton NMR have revealed that the SO_4^{-2} reorientation is in a time scale of 10^{-4} s around 300 K and that this correlation time it is claimed to obey Arrhenius relation. The inverse of this correlation time is of the same order as the relaxation frequencies that we have measured in phase II of $RbHSeO_4$.

The dielectric relaxations in MH_2PO_4 (M=K, NH_4), L_2SO_4 (L=K, Li, Cs, Na) and $CsHSeO_4$ [19-25] are characterized by both σ_o and $f_{\max}$ (the characteristic relaxation frequency) being thermally activated with about the same activation energy, indicating that mobile ions seem to be responsible also for the relaxation. Based on this, and considering the discussed results for acid selenates and sulphates, we are proposing that this dielectric relaxation in $RbHSeO_4$ could be due to H^+ jump and SeO_4^{-2} reorientation changing of the local lattice polarizability inducing dipoles. That is, the reorganization of the structural pattern or environment (*e.g.*, phosphate or sulphate or selenate reorientation) is an inherent part of the mobile ion diffusion path. As a result, because lattice polarizability configuration such as $HSeO_4^-$ may be formed and the observed relaxation can correspond to H^+ local jumps or SeO_4^{-2} reorientations, we do believe that this kind of relaxation may occur in $RbHSeO_4$ at lower frequencies.

4. Conclusions

The frequency and temperature dependence of the permittivity data for $RbHSeO_4$ clearly show a very slow dielectric relaxation, at around 385 Hz at 310 K, which shifts to higher frequencies ($\sim$40 kHz) as the temperature increases. We suggest that, by increasing the temperature of $RbHSeO_4$ the hydrogen bonds become progressively weaker such that the protons start to jump from one site to another site and the selenate tetrahedra adopt new reorientations that cause structural distortion in the corresponding sublattice, thus creating nonzero polarization due to induced dipole-like moments. In other words, due to H^+ jump, local molecular configurations such as $HSeO_4^-$ may be formed resulting in a dielectric relaxation at lower frequencies similar to those observed in MH_2PO_4 (M=K, NH_4), L_2SO_4 (L=K, Li, Cs, Na) and $CsHSeO_4$ in the 10^4-10^6 Hz frequency range. The relaxation frequency is thermally activated with an activation energy E_a= 0.9 eV which is in close agreement with that associated with transport of charge carriers.

Acknowledgements

The authors would like to acknowledge the support of the Banco de la República de Colombia and Grupo de Física Aplicada III, Universidad Complutense de Madrid.

1. F. A. Cotton, B. A. Frenz, and D. L Hunter, *Acta Cryst. B* **31** (1975) 302.
2. Y.N. Moskvich, O.V. Rozanov, A.A. Sukhovsky, and I.P.Aleksandrova, *Ferroelectrics* **63** (1985) 83.
3. O.V. Rozanov, Y.N. Moskvich, and Sukhovskii, *Sov. Phys. Solid State* **25** (1983) 212.
4. Y.N. Moskvich, A.A. Sukhovskii, and O.V. Rozanov, *Sov. Phys. Solid State* **26** (1984) 21.
5. A. Waskowska, S. Olejnik, and K. Lukaszewicz, *Acta Cryst. B* **34** (1978) 3344.
6. A. Waskowska, S. Olejnik, K. Lukaszewicz, and Z. Czapla, *Cryst. Struct. Comm.* **9** (1980) 663.
7. I. Brach, D.J. Jones, and J. Roziere, *J. Solid State Chem.* **48** (1983) 401.
8. I.P. Makarova, E.E. Rider, V.A. Sarin, I.P. Aleksandrova, and V.I. Simonov, *Sov. Phys. Cristallogr.* **34** (1989) 510.
9. J. Majszczyk, J. Raczka, and Z. Czapla, *Phys. Status Solidi (a)* **67** (1981) K123.
10. I.P. Aleksandrova, O.V. Rozanov, A.A. Sukhovsky, and Y.N. Moskvich, *Phys. Letters* **95A** (1983) 339.
11. Z. Czapla, T. Lis, L. Sobczyk, and A. Waskowska, *Ferroelectrics* **26** (1980) 771.
12. R. Poprawski, J. Mroz, Z. Czapla, and L. Sobczyk, *Acta Phys. Pol. A* **55** (1979) 641.
13. J. Kroupa, and Z. Czapla, *Ferroelectrics* **25** (1980) 597.
14. Yves Luspin, Yann Vaills, and Georges Hauret, *Solid State Communications* **87** (1993) 523.
15. J. C. Badot. A. Fourier-Lamer, N. Baffier, and Ph. Colomban, *J. Phys.* (Paris) **48** (1985) 1327.
16. J. C. Badot. A. Fourier-Lamer, N. Baffier, and Ph. Colomban, *Solid State Ionics* **28-30** (1988) 1617.
17. J. C. Badot, and Ph. Colomban, *Solid State Ionics* **35** (1989) 143.
18. Ph. Colomban, and A. Novak, *J. Mol. Struct.* **177** (1988) 277.
19. J. E. Diosa, R. A. Vargas, I. Albinson, and B.-E. Mellander, *Phys. Stat. Sol. (b)* **241** (2004) 1369.
20. J. E. Diosa, R. A. Vargas, I. Albinson, and B.-E. Mellander, *Solid State Communication* **132** (2004) 55.
21. J. E. Diosa, R. A. Vargas, I. Albinson, and B.-E. Mellander, *Solid State Communication* **136** (2005) 601.
22. J. E. Diosa, R. A. Vargas, M. E. Fernández, I. Albinsson, and B.-E. Mellander, *Physics Status Solidi (c)* **2** (2005) 3714.
23. J. E. Diosa, R. A. Vargas, I. Albinson, and B.-E. Mellander, *Ferroelectrics* **333** (2006) 253.
24. J. E. Diosa, Peña Lara. D, and R. A. Vargas, *Journal of Physics and Chemistry of Solids* **74** (2013) 1017.
25. O. Checa, J.E. Diosa, R.A. Vargas, and J. Santamaria, *Solid State Ionics* **180** (2009) 673.
26. C. Elissalde, and R. Ravez, *J. Mater. Chem* **11** (2001) 1957.
27. K. Funke, and R. D. Banhatti, *Solid State Ionics* **177** (2006) 1551.
28. A. K. Jonscher, *Universal Relaxation Law*, (Chelsea Dielectric Press, London, 1996) p. 143.
29. M. Mizuno, and S Hayashi, *Solid State Ionics* **167** (2004) 317.
30. S. Hayashi, and M. Mizuno, *Solid State Ionics* **171** (2004) 289.